Article

Not peer-reviewed version

Bioresponsive Gelatin-Hyaluronic Acid Hydrogels for 3D Bioprinting

Mst Rita Khatun , Amitava Bhattacharyya , Maral Gunbayar , Minsik Jung , Insup Noh *

Posted Date: 29 June 2023

doi: 10.20944/preprints202306.2020.v1

Keywords: Bioresponsive; gelatin; hyaluronic acid; bioprinting; cell-delivery; tissue engineering

Article

Bioresponsive Gelatin-Hyaluronic Acid Hydrogels for 3D Bioprinting

Mst Rita Khatun [1], Amitava Bhattacharyya [1,2,3], Maral Gunbayar [1], Minsik Jung [1] and Insup Noh [1,3]*

[1] Department of Chemical and Biomolecular Engineering, Seoul National University of Science and Technology, Seoul 01811, Republic of Korea
[2] Functional, Innovative and Smart Textiles, PSG Institute of Advanced Studies, Coimbatore 641004, India
[3] Convergence Institute of Biomedical Engineering and Biomaterials, Seoul National University of Science and Technology, Seoul 01811, Republic of Korea
* Correspondence: insup@seoultech.ac.kr

Abstract: Development of bioresponsive extrudable hydrogels for 3D bioprinting is imperative to address the growing demand for scaffold design and efficient and reliable methods of tissue engineering and regenerative medicine. This study proposed genipin-crosslinked gelatin-hyaluronic acid hydrogel bioink with different amounts of gelatin tailored for 3D bioprinting, focusing on high cell density loading and less artificial extracellular matrix (ECM) effect, as well as exploring their potential applications in tissue engineering. The bioresponsiveness of these hydrogel scaffolds was successfully evaluated in different physiological conditions. 3D and four-axis printing of complex structures such as shapes of hollow tube, star, pyramid, and four-axis tubular scaffolds prove the hydrogel's high extrusion ability and post-printing shape fidelity. Cytocompatibility and high cell density 3D bioprinting using this moderately stable hydrogel exhibit high potential for precise cell-delivery modes in tissue engineering as well as regenerative medicine.

Keywords: bioresponsive; gelatin; hyaluronic acid; bioprinting; cell-delivery; tissue engineering

1. Introduction

3D Bioprinting is widely used in tissue engineering and regenerative medicine for fabricating complex artificial tissue and organ structures that can mimic natural tissues and organs [1]. As the success of tissue formation depends on the nature of bioinks used in 3D bioprinting, various polymeric hydrogels have been studied in response to the increasing significance of 3D bioprinting and injectable hydrogels in these fields [2]. The physical, chemical, and biological properties of polymeric hydrogels vary widely depending on their biomedical application areas, including tissue engineering scaffolds, biosensors, burn dressings, drug delivery, cell encapsulation as well as bioprinting. Most of biodegradable hydrogels for tissue engineering scaffolds and biosensors may not be suitable for bioprinting, requiring a better understanding of the advantages and weaknesses of the fabricated hydrogels for various applications [3].

A new class of hydrogel, named bioresponsive hydrogels, has gained researchers' interest in diagnostics, drug delivery, and tissue regeneration/wound healing [4]. Bioresponsive hydrogels respond to external stimuli or stimulate specific biological signals through natural biological processes [5]. These bioresponsive hydrogels change their physico-chemical and biological properties over time and spatio-temporal due to swelling, collapse, or degradation in response to selective biological environments [6]. Bioresponsive hydrogels are under extensive research for targeted cell delivery, cancer therapy, drug delivery as well as 3D bioprinting systems with and without scaffolds [7–9]. Scaffold-based and scaffold-free 3D cell culture systems have been developed to establish related *in vitro* models replicating the complex structure observed *in vivo* [10]. Scaffold-based cell-embedded 3D bioprinting systems often suffer a limitation of less cell communication as well as difficulty in matching the time for scaffold degradation and tissue regeneration, especially in slow degradation biomaterials [11]. This can be addressed using high-density 3D bioprinting of hydrogels

 doi:10.20944/preprints202306.2020.v1

and controlled degradation of the biomaterials to generate better cell-cell interactions, important for the functioning of the artificial neo tissue. High cell density and less amount of hydrogel minimize the effect of artificial extracellular matrix leading to a close replica of the natural tissues [12].

Several natural biomaterials are used in fabricating bioresponsive extrudable hydrogel for 3D bioprinting. Gelatin, derived from denatured collagen, is a commonly employed biopolymer for hydrogel formation, finding wide application in pharmaceuticals, food, medical, and tissue engineering fields [13]. Gelatin-based hydrogels possess several favorable characteristics, including biocompatibility, non-toxicity, non-immunogenicity, biodegradability, cost-effectiveness, and easy accessibility. These qualities make them highly suitable materials for various biomedical applications [14]. However, the gel formed through the physical crosslinking of gelatin lacks structural stability and quickly dissolves when exposed to high temperatures [15]. The mechanical and physical properties of gelatin hydrogel can be improved by addition of other polymers and chemical crosslinking. Hyaluronic acid (HA, also known as hyaluronan), a key component of skin and cartilage, is one of the important biomaterials for biocompatible gel, which is an anionic, non-sulfated glycosaminoglycan made up of repeating units of D-glucuronic acid and N-acetyl-D-glucosamine. It is found in all connective, epithelial, and neural tissues [16–19]. In recent years, HA has been functionalized with natural polymers, synthetic polymers, or nanoparticles in the form of composite materials, hydrogels, or hydrogel nanocomposites [20,21]. Genipin has been employed as a strong yet safe crosslinker of proteins like collagen, gelatin, and polysaccharide such as chitosan. This is preferred for crosslinking bioink polymers during 3D bioprinting as it possesses some anti-inflammatory qualities [14].

In this present study, gelatin-HA-based bioresponsive hydrogel crosslinked with genipin is proposed for 3D bioprinting of tissue engineering scaffolds with high shape fidelity and high resolution. Here, positively charged Type-A gelatin (isoelectric point in the region of 7.0 ~ 9.5) is used to improve the polyelectrolyte complex formation with negatively charged HA. Genipin crosslinking with gelatin molecules gives further stability and extrudable properties for the hydrogel. This hydrogel is expected to be stable at room temperature while its stability (bioresponsiveness) needs to be assessed in physiological conditions such as body temperature and pHs. Three different amounts of gelatin were used to prepare gelatin-HA hydrogel in fixed amount of HA (1 g, 1.2 g, and 1.5 g gelatin, each with 0.3 g HA in 20 ml distilled water, coded as Gel 1, Gel 2, and Gel 3, respectively) crosslinked with genipin (5 mg). Figure 1 shows the present study scheme of the 3D bioprinting with this extrudable gelatin-HA acid hydrogel. Analysis of hydrogel's rheological and mechanical properties, high-resolution 3D printing as well as four-axis printing, and cytocompatibility study are carried out using this bioresponsive hydrogel. High cell density is used in the gelatin-HA hydrogel for 3D bioprinting. During and after the degradation of this hydrogel scaffold, cell-to-cell interaction would be increased in this 3D bioprinting system, leading to better functional tissue formation by minizing scaffold effects.

Preprints (www.preprints.org) | NOT PEER-REVIEWED | Posted: 29 June 2023 doi:10.20944/preprints202306.2020.v1

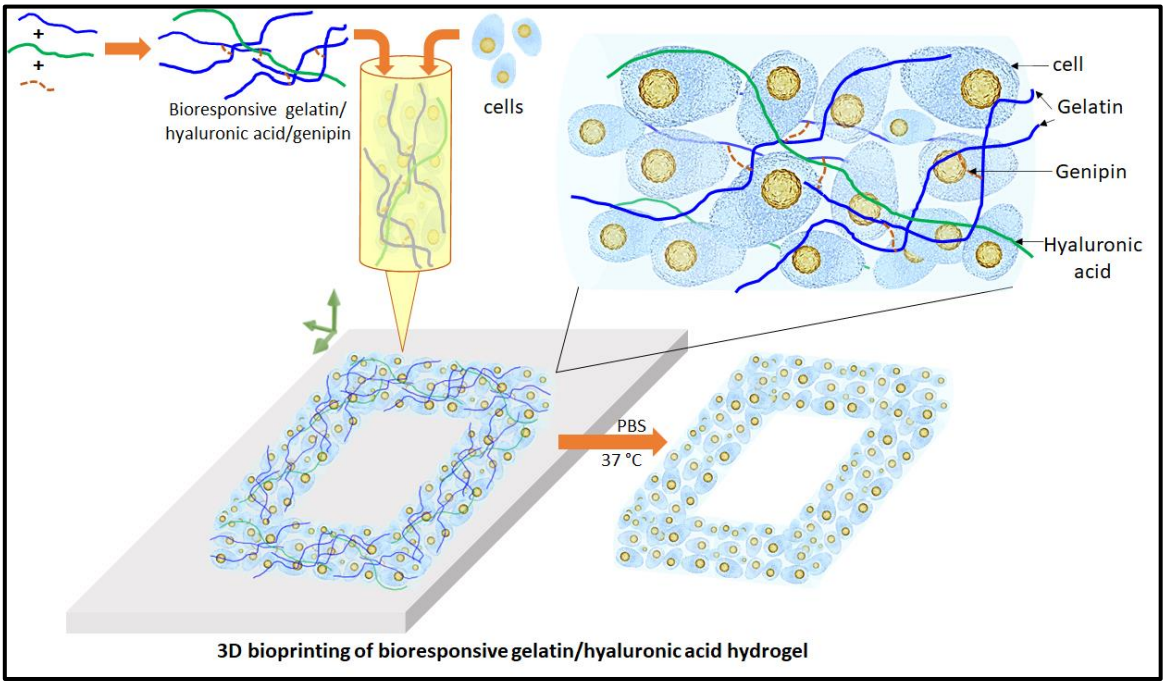

Figure 1. Scheme of 3D bioprinting with bioresponsive gelatin-hyaluronic acid hydrogel.

2. Results and Discussion

2.1. Gelatin-HA hydrogel formation and it's bioresponsiveness

The process of gelatin-HA hydrogel formation is sequentially in two stages: firstly, polyelectrolyte complexing and then by genipin crosslinking with gelatin as proposed in Figure 2a. The bonding of gelatin with negatively charged HA through polyelectrolyte complex formation is better initiated at lower pH. Hence, the Type-A gelatin, which has higher isoelectric point (isoelectric point at around 7.0 ~ 9.5) than Type-B with that at 4.7 ~ 5.3, is selected in this study. Below the isoelectric point, gelatin is positively charged and the bond formation with HA is expected to be more stable. In the cross-linking process using genipin, the amine group's free electrons in gelatin polymer initiate a nucleophilic attack on the nearby hydroxyl group of genipin's ether group with unsaturation, leading to the opening of the cyclic structure and the formation of an intermediate aldehyde group (Figure 2-a). This intermediate aldehyde group then reacts with the amine group, forming an intermediate nitrogen-containing ring structure. Furthermore, the free electron on the gelatin amine group reacts with the ester group at the upper end of genipin, resulting in the formation of an amide bond. This amide bond contributes to both intramolecular and intermolecular cross-linking of gelatin newtork. FTIR spectra in Figure 2b showed characteristics peaks of HA at 3401, 1615 and 1450 for stretching vibration of O-H / N-H group, C=O group and C-O bonds of -COO- group, respectively [22]. The presence of water (O-H stretching) and amide A resulted in a band at 3316 cm^{-1} in the FTIR of gelatin chemical structure (Figure 2b_{ii}). The presence of amide-I in gelatin was confirmed by the peak at 1636 cm^{-1} [23]. The FTIR analysis of genipin revealed specific absorption peaks at different wavelengths. One peak at 1680 cm^{-1} was associated with the stretching vibrations of the carboxymethyl group (C=O), while another peak at 1620 cm^{-1} was related to the C=C vibration of the olefin ring in genipin. The presence of a double peak at 3412 cm^{-1} in the genipin spectrum was likely due to the overlapping of vibrations from aromatic carbon-hydrogen (C–H) bonds and hydroxyl (O–H) groups [24]. The FTIR spectrum of hydrogel demonstrates the presence of the cross-linking amide bond (-CONH-) at approximately 1530 and 1632 cm^{-1}, confirming the strong association between the gelatin and genipin, which aligns with the previously described reaction mechanism in Figure 2-a.

Preprints (www.preprints.org) | NOT PEER-REVIEWED | Posted: 29 June 2023 doi:10.20944/preprints202306.2020.v1

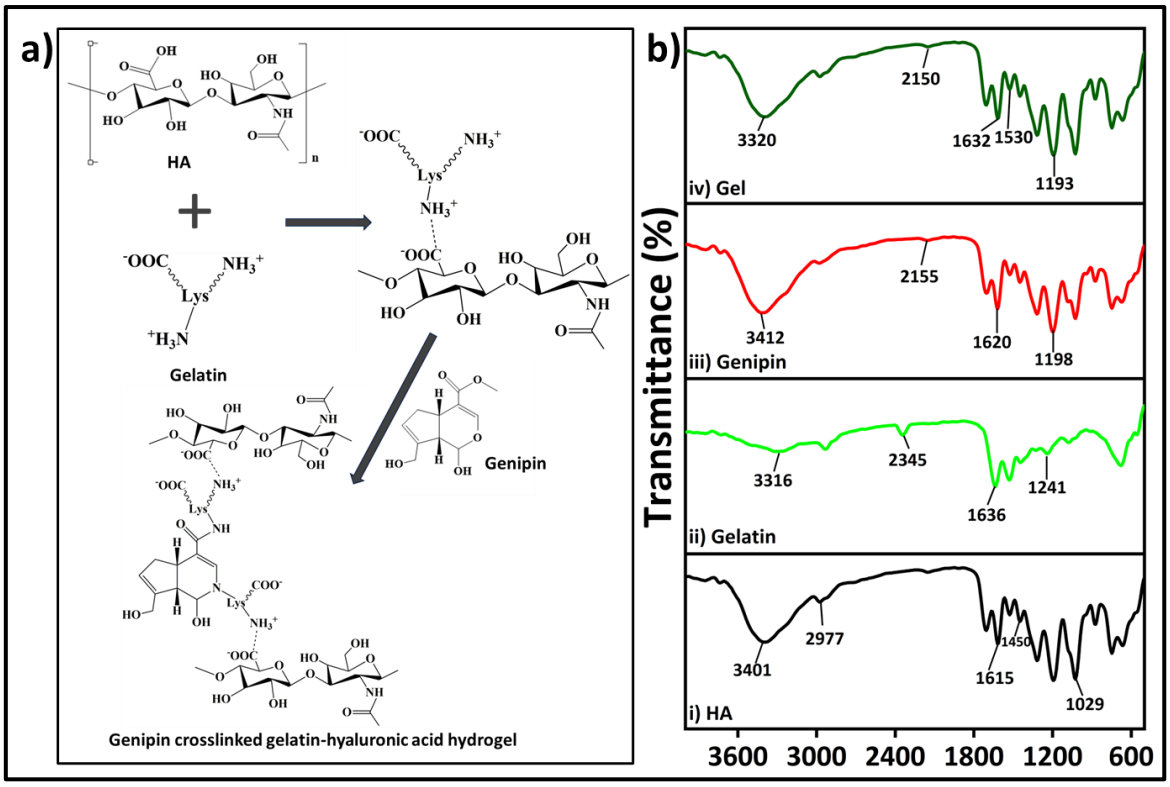

Figure 2. (a) Proposed reaction mechanism of the gelatin-HA gel formation with genipin, (b) FTIR analysis of hyaluronic acid (HA); gelatin, genipin, and gel (i, ii, iii, iv respectively).

The bioresponsiveness of these three different gelatin-HA hydrogels has been studied at different temperature and pH. Figure 3 represents the swelling and degradation of the different composition of gels into phosphate buffer saline, pH 7.4 at 37°C and room temperature. From Supporting Figure 1, all these three different gelatin-HA hydrogels were swelled for the first 6 hours due to the gelling property of these crosslinked hydrogels. After that the gels started degrading, and within 48 hours Gel 3 is completely degraded away. After 48 hours, Gel 1 and Gel 2 have some portion remaining after degradation. As other than gelatin, the amounts of all components including crosslinker genipin are constant in all hydrogel compositions. The increased amount of gelatin reduces crosslinking sites of the hydrogel making it more vulnerable for temperature and ion induced degradation. At room temperature all the three compositions of gels didn't degrade away after 48 hours. Supporting Figure 2 shows the swelling and degradation of the three compositions of hydrogels in different pH (pH 2.5 and pH 9) at 37°C. There was no swelling or degradation observed in all these three conditions hydrogel after 48 hours into acidic media and Gel 1 and Gel 2 remained stable after 5 days (Supporting Figure 3).

Preprints (www.preprints.org) | NOT PEER-REVIEWED | Posted: 29 June 2023 doi:10.20944/preprints202306.2020.v1

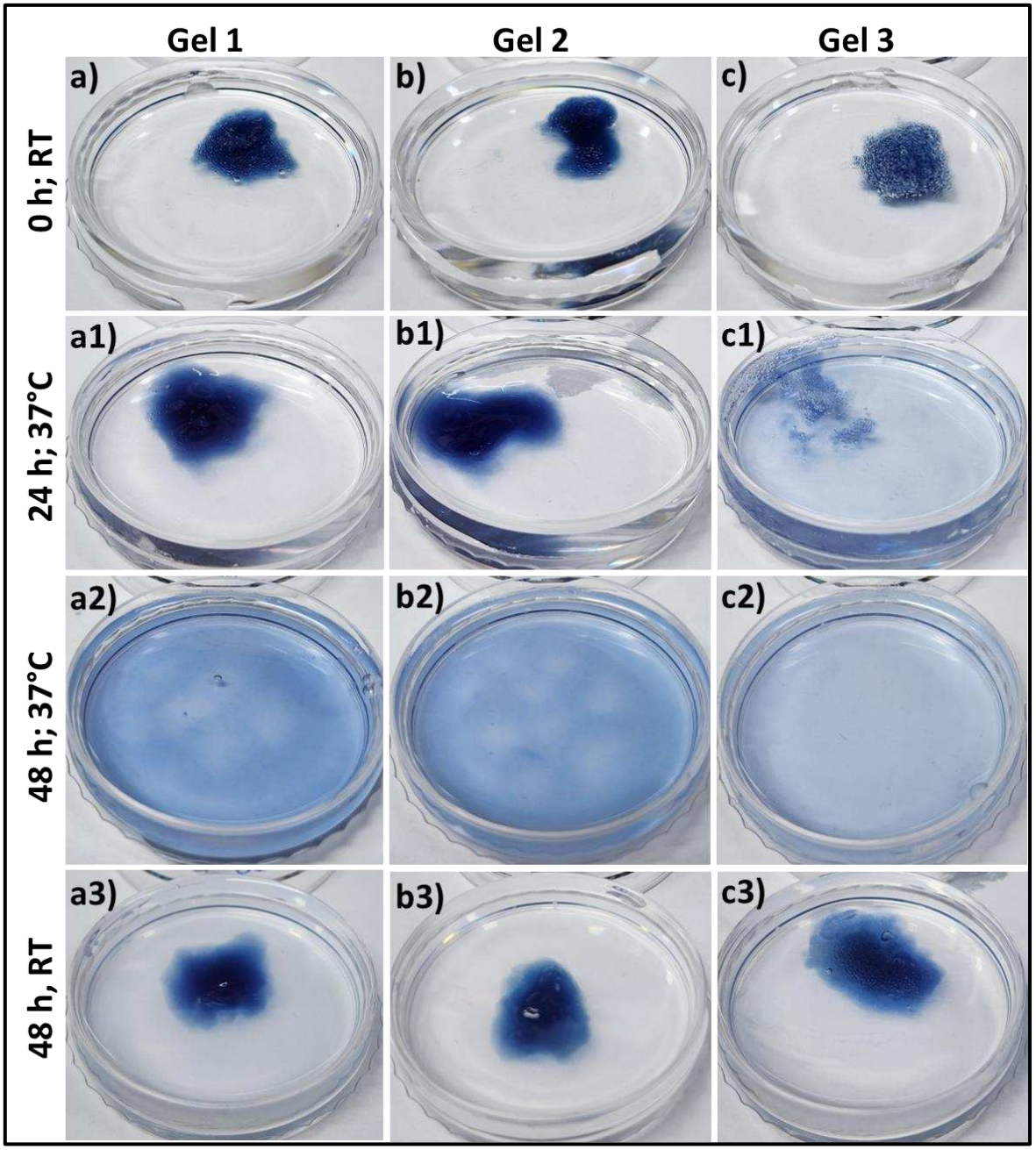

Figure 3. Swelling & degradation study of different gelatin-HA hydrogels at 37°C and room temperature into phosphate buffer, pH 7.4 for 48 hours. (a-c2) at 37°C; (a3-c3) at room temperature after 48h.

In alkaline media, all the gels swelled first, and Gel 3 completely degraded within 48 hours. Gel 2 almost degraded away and Gel 1 degraded very less. The very less degradation under acidic condition may be justified by strong polyelectrolyte bonding between type A gelatin and HA. Type A gelatin provides more positive charge in acidic buffer media because of its high isoelectric point which makes the bond stronger with negatively charged HA. These data successfully prove the bioresponsiveness of these hydrogels.

2.2. Rheological and mechanical properties of the gelatin-HA hydrogels

Rheological properties analysis of gelatin-HA hydrogels involves the study of their flow and deformation characteristics under various conditions. It plays an important role in understanding the behavior of hydrogels which are composed mostly of water. Viscosity is an important rheological property which refers to the resistance of a material to flow. It is an essential property to study in hydrogels as it determines their ability to flow or deform under applied stress. Figure 4a depicts the

Preprints (www.preprints.org) | NOT PEER-REVIEWED | Posted: 29 June 2023 doi:10.20944/preprints202306.2020.v1

rheological property analysis of the three different compositions of the hydrogels. Parallel plate rotating discs were used to study the rheological behavior of bioink. This study method is recognized by the researchers to comprehend the rheology of bioink for extrusion based 3D bioprinting [25]. The viscosity of the gels increased as the gelatin concentration increased, and the samples showed shear-thinning behavior. The shear-thinning property of gels would facilitate their bioprinting with high resolution and structural integrity.

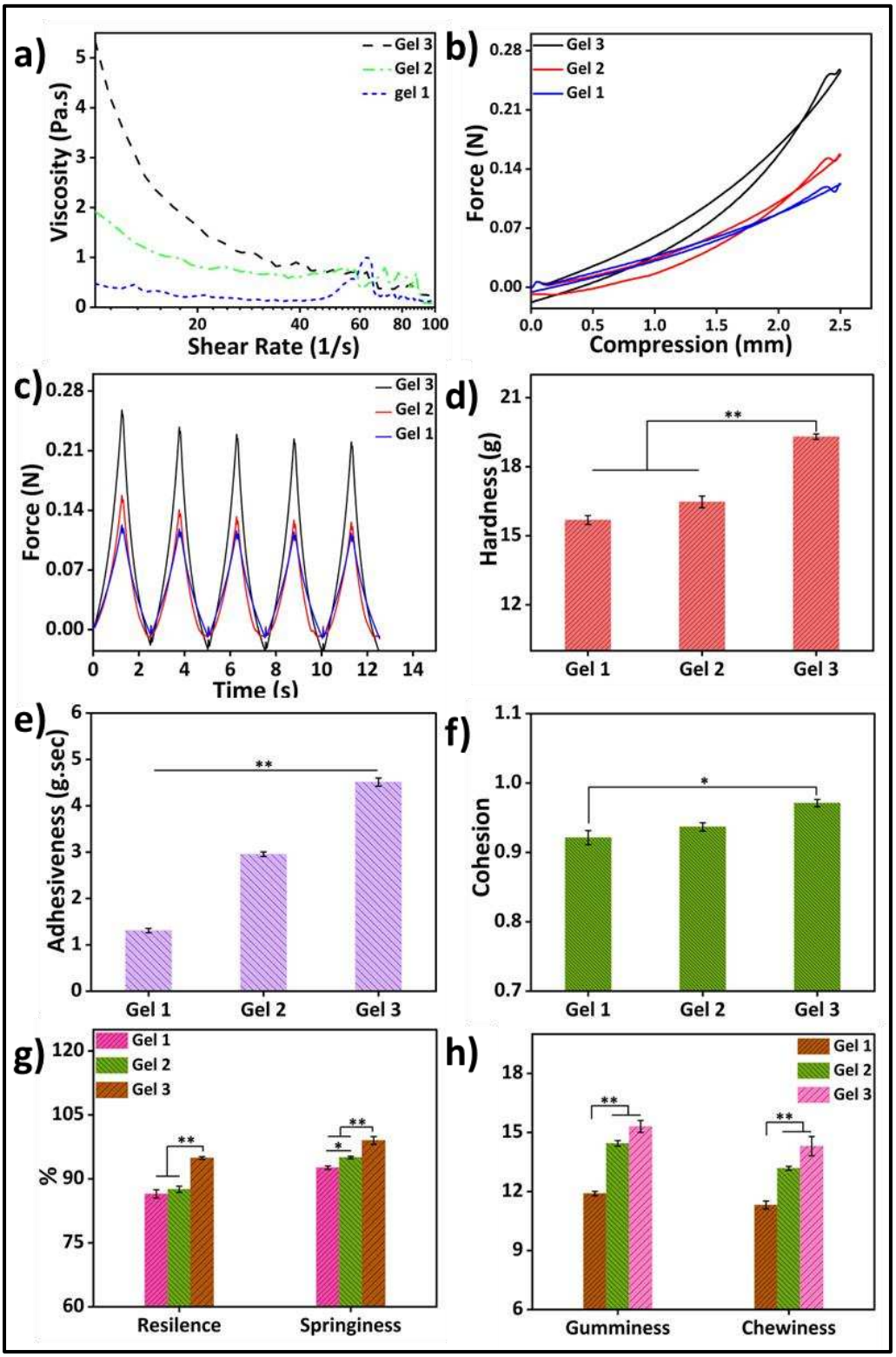

Figure 4. (a) Rheological properties analysis of three different gelatin-HA hydrogels; Cyclic compressive response of the hydrogels (b) with compression; (c) with time; Mechanical properties analysis of three

 doi:10.20944/preprints202306.2020.v1

different hydrogels (d) Hardness; (e) Adhesiveness; (f) Cohesion; (g) Resilience & Springiness; (h) Gumminess & Chewiness.

A texture analyzer was used to study the cyclic compressive mechanical properties (Figure 4b–h). The cyclic compressive strengths and mechanical properties of the higher gelatin-containing samples were significantly higher among the three different samples. This may be because of the higher mass content in the hydrogel with increasing amounts of gelatin. For the same volume of the hydrogel, only the gelatin quantity increased to get better stability as well as physical, mechanical, and biological properties. Several researchers have reported that increasing the quantity of gelatin in hydrogels leads to improved mechanical strength and enhanced adhesiveness, as indicated by a greater negative load region during retraction. Hardness reflects the gel's strength, while gumminess and chewiness represent its crunching properties. Adhesiveness refers to the gel's ability to attach to other surfaces, while cohesiveness indicates its strength in maintaining its own structure. Springiness indicates the material's capacity to return to its original shape, while resilience measures the energy loss during deformation. Controlling these properties, including hardness, cohesiveness, adhesiveness, chewiness, and gumminess, is crucial for hydrogels to enhance printability and mechanical properties in 3D bioprinting applications. Several studies have highlighted the use of higher amounts of gelatin to achieve these improvements.

2.3. Morphology of the gelatin-HA hydrogels

Scanning electron spectroscopy (SEM) analysis allows for high-resolution imaging of the hydrogel surface, providing information about its morphology, roughness, and surface features. It helps to observe the microstructure of the gelatin-HA hydrogel, such as the presence of pores, surface irregularities, or surface modifications. The surface morphology is very important for applications in tissue engineering, where cell adhesion and growth are influenced by surface characteristics. Again, from the SEM of the cross-sections, the internal structure of the hydrogel, including pore distribution, interconnectivity, and homogeneity can be analyzed. This information is crucial for understanding the transport properties of the hydrogel, such as diffusion of nutrients, drugs, or bioactive molecules within the hydrogel. SEM analysis was carried out to check the structural changes of the four different conditions gels with the increase of gelatin content. From Figure 5(a-c1), SEM images revealed a porous surface and cross-section structure of the three different gelatin-HA hydrogels. SEM images clearly showed that the porosity sharply decreased with the increase of gelatin amount in the hydrogel which proves the structural compactness of the of the high gelatin containing hydrogel. Gel 1 showed higher porous surface and cross section morphology of the hydrogels than Gel 2 and Gel 3. The uniform pore distribution and higher porous structure proves the hydrogels well and fully crosslinked gel network. Again, with the increase of gelatin amount in the hydrogel, the porosity decreased, and pore size increased which proves the less crosslinking density in the hydrogel. From the figure, Gel 1 is fully crosslinked and after that the genipin amount was insufficient to crosslink the higher amount of gelatin which is responsible for less and irregular surface and cross section morphology of the hydrogel.

Preprints (www.preprints.org) | NOT PEER-REVIEWED | Posted: 29 June 2023 doi:10.20944/preprints202306.2020.v1

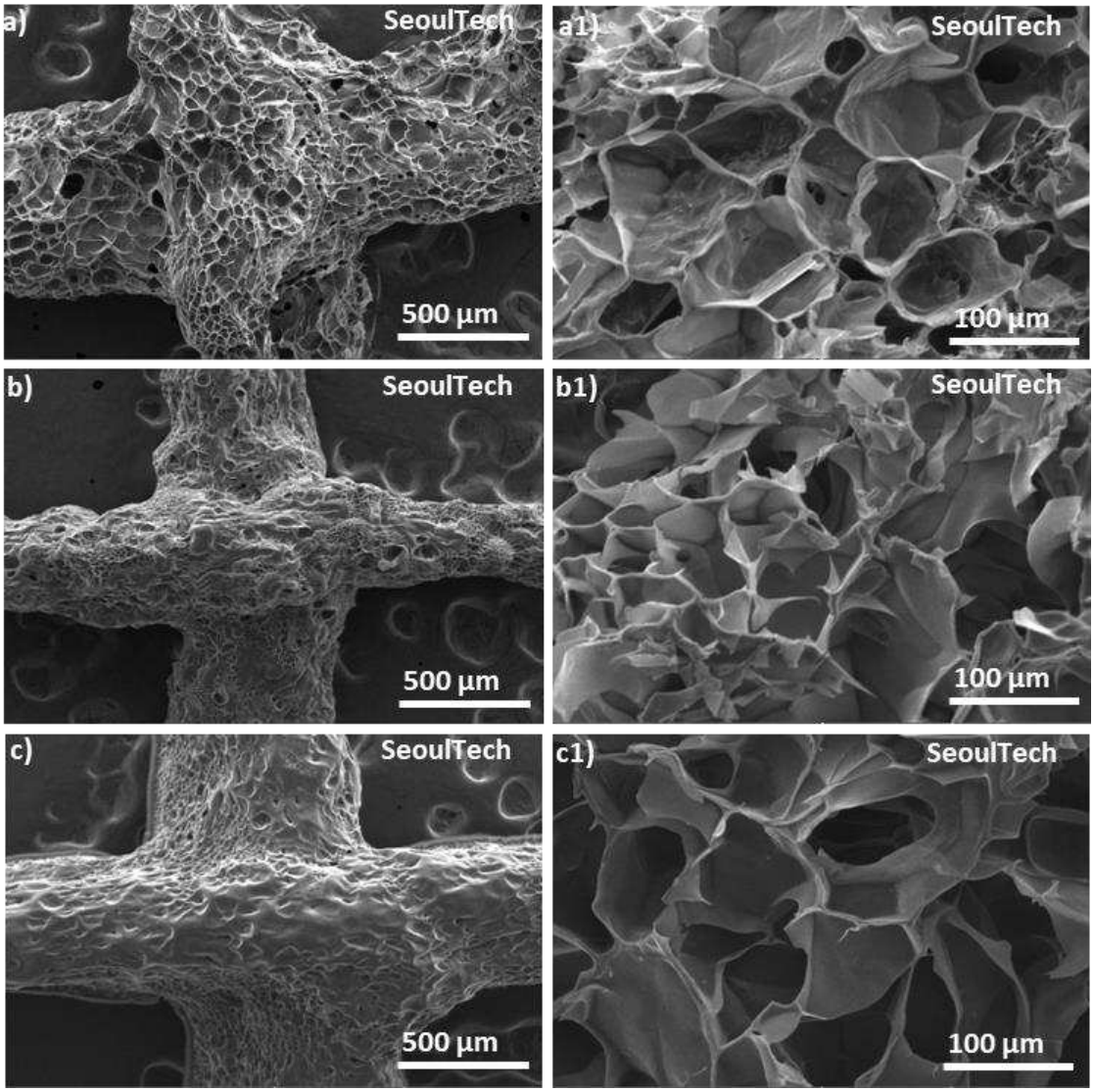

Figure 5. SEM images of the surface and cross-section of the three different gelatin-HA hydrogels. Surface and cross-section image of Gel 1 (a, a1); Gel 2 (b, b1); Gel 3 (c, c1) respectively.

2.4. 3D printability of the gelatin-HA hydrogels for complex structures

The hydrogels exhibit a shear-thinning property, which means that they can easily flow and be extruded during the pneumatic-based extrusion 3D printing process. The parameters such as nozzle speed, pressure, and diameter were carefully optimized to ensure optimal printing conditions. After analysis of physical properties and extrusion ability, Gel 1 optimized for 3D printing as well as four-axis printing. Using these optimized parameters, various shapes were successfully printed, including hollow tubes and star shapes, each composed of approximately 50 layers and reaching a height of 1cm (Figure 6a, b). Upon lyophilization, SEM images (Figure 6 a1, a2, b1, b2) revealed a porous surface morphology in these complex printed shapes. The 3D printed structures made from gelatin-HA gels, particularly a pyramid-like structure (Figure 6c, 1.5 cm height and around 100 layers), exhibited exceptional stability and maintained their shape fidelity after printing. An interesting observation was that the printed structures firmly adhered to the substrates without the need for any additional glue or adhesive, highlighting the high adhesiveness of the hydrogel to glass substrates. Even when the 3D printed samples were inverted multiple times with the substrate, the structures remained intact and did not break or detach (Supporting Figure 4). In brief, the hydrogels with shear-thinning properties demonstrated excellent extrudability and printability in a pneumatic-based extrusion 3D printer. The optimized parameters allowed the successful printing of different shapes, and the resulting printed structures exhibited a porous morphology. Notably, the printed structures

Preprints (www.preprints.org) | NOT PEER-REVIEWED | Posted: 29 June 2023 doi:10.20944/preprints202306.2020.v1

exhibited remarkable stability, maintained their shape fidelity, and firmly adhered to glass substrates without additional adhesives, indicating the high adhesiveness of the hydrogel. The robustness of the printed structures was evident as they remained intact even after repeated inversions with the substrate.

The hydrogel was successfully used for four-axis printing, as shown in Figure 6d and d1. This printing technique involved utilizing a rotating plastic tube connected to an RPM controller as a substrate platform. By editing the G-codes, the rod's movement in the X and Y axes was controlled while maintaining a constant syringe height. The G-codes were adjusted to achieve a diamond-like porous structure in the tubular constructs. During the printing process, the circular substrate moved horizontally back and forth, as demonstrated in Supporting Video 1. A crucial aspect to consider here is the cohesive and adhesive properties of the gels during the rotation of the plastic tube substrate during 3D printing. The gel needed to possess both self-cohesiveness and adhesion to the plastic surface to form a tubular shape that could resist falling from the hydrophobic inert surface. Insufficient cohesion and adhesion would lead to unstable printed layers, potentially causing the structure to collapse while rotating the polypropylene tube substrate. Therefore, the gel's cohesive and adhesive characteristics played a vital role in maintaining the stability of the printed layers and structures.

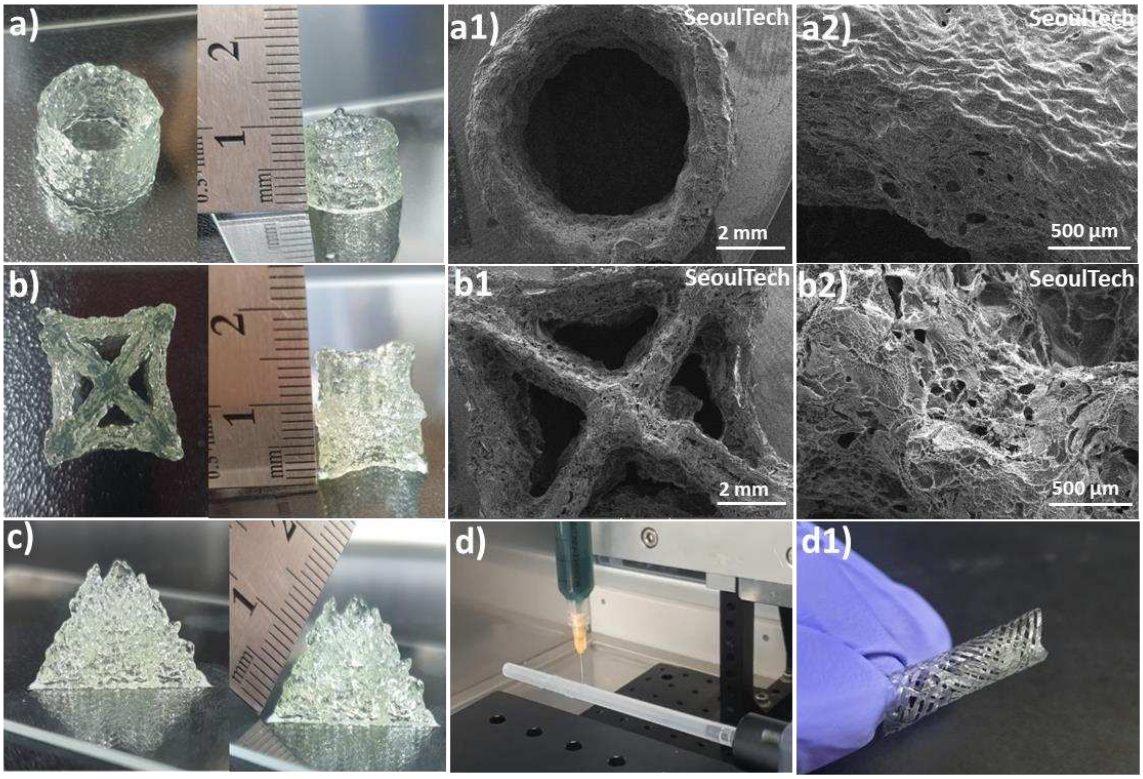

Figure 6. 3D and four-axis printing of complex structures with gelatin-HA gel. (a, a1, a2) Digital and SEM images of Hollow tube; (b, b1, b2) Digital and SEM images of Star shape; (c) Pyramid shape; (d, d1) Four-axis printed tubular shape.

After printing, the constructs were washed with distilled water (DW) and air-dried. The samples exhibited a high level of shape fidelity and stability. The flexibility of the printed constructs can be observed in Supporting Video 2. Additionally, by adjusting the dimensions and compositions of the bioink, the resolution and size of the printed structures can be modified or scaled to suit specific applications. This approach can also be extended to the development of nerve conduits using different electroconductive biomaterials, bone tissue engineering scaffolds, or stents. These experiments effectively demonstrate the capability of bioink gels to efficiently print various intricate and self-supporting large structures within a short timeframe and with high repeatability.

 doi:10.20944/preprints202306.2020.v1

2.5. Cell culture studies on 3D bioprinted gelatin-HA hydrogels

Figure 7 presents the results of in vitro cell study using mouse osteoblast MC3T3 cells. Genipin is a strong but safe substance that can bind proteins like chitosan, collagen, and gelatin together. Recent studies have shown that when genipin is added to these materials, it gives them anti-inflammatory properties [26]. Genipin was suggested long back as a substitute for glutaraldehyde, a fixative for biological tissues [27]. It was proven to be significantly less toxic, about 10,000 times, while being nearly as effective as glutaraldehyde. The MTT assay (Figure 7a) was performed for up to day 3, and all samples exhibited cell viability exceeding 70%, indicating that the hydrogels used in this study are supportive of cell growth and non-toxic [15,22]. The MTT assay involved extracting substances from the cell-encapsulated hydrogels for analysis. The cell viability increased over time in all samples, suggesting that the hydrogels are non-toxic. The bioink used in this study for crosslinking the biocompatible components did not contain any toxic substances.

Figure 7 (b, b1, c, c1) showed the DAPI stained images of blue nucleus at day 0 & day 3. The 3D bioprinted grid like structure preserves after degradation of the hydrogel components as shown in low magnification Day 3 DAPI image (Figure 7 c). The cells covered the entire structure. The day 3 live and dead (LnD) result reveals cell-to-cell communication after the complete degradation of ECM (Figure 7 c2). Furthermore, the cytoskeletons of the cells exhibit a spread morphology and improved structural strength after three days of culture. The live/dead results (Figure 7 b2) at Day 0 showed that the live cells were evenly distributed within the gel matrix. The three-day study further confirmed that these hydrogels are supportive of cell growth. The high-density 3D bioprinted structure demonstrated consistent cell-delivery for scaffold formation upon the complete degradation of the ECM. Within three days (Figure 7 c2), the gel matrix completely degraded, the cells multiplied as well as cell to cell communication increased and formed scaffold shape tissue. High magnifications images of LnD and DAPI/actin from Figure 8 clearly shows the excellent cell-to-cell communication established after degradation of the hydrogel. This has the possibility to lead fully functional tissue formation using this method of high density 3D bioprinting with the studied gelatin-HA hydrogel.

Preprints (www.preprints.org) | NOT PEER-REVIEWED | Posted: 29 June 2023 doi:10.20944/preprints202306.2020.v1

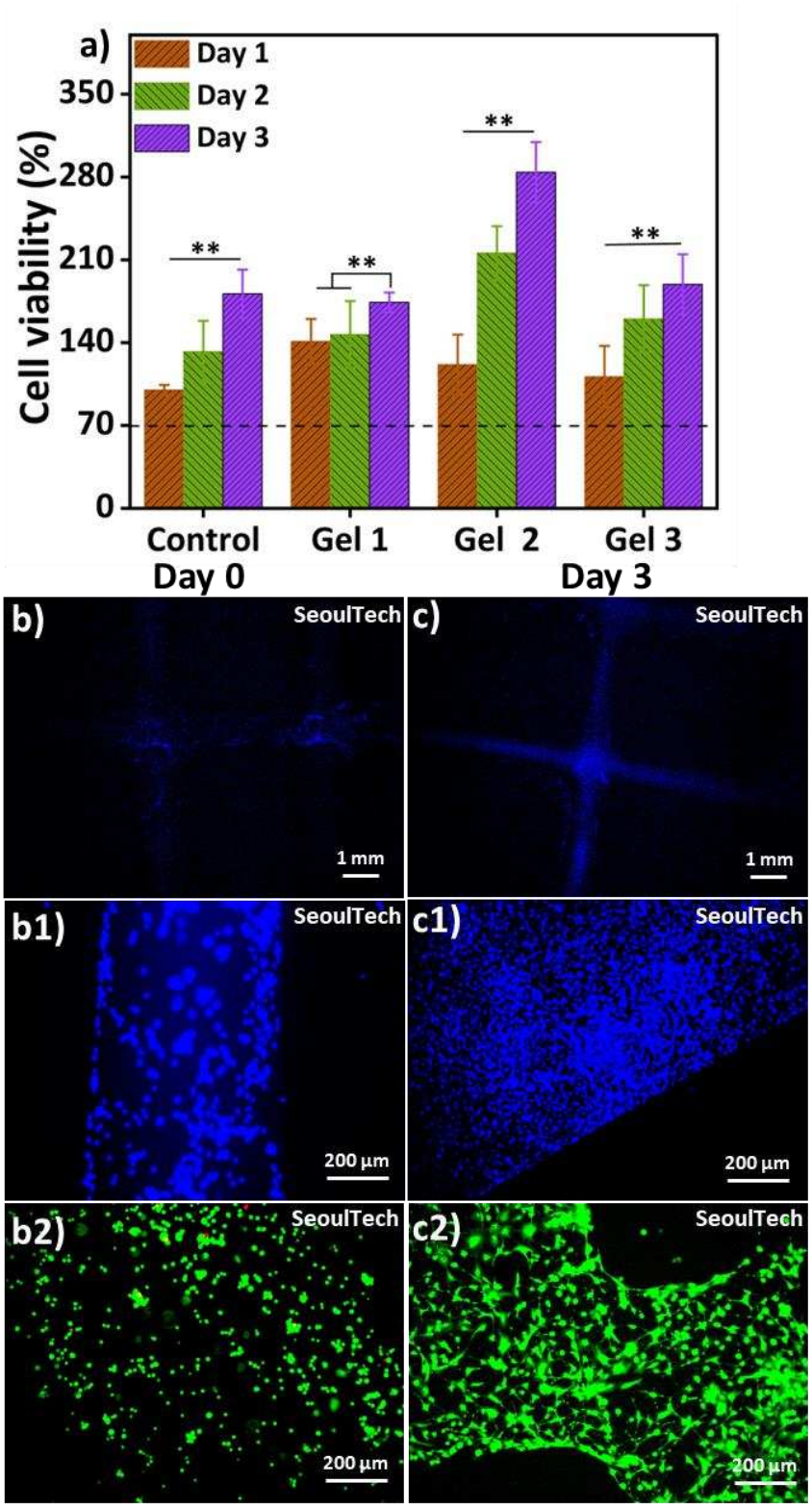

Figure 7. (a) MTT assay of three different conditions hydrogel; (b, c) DAPI staining low magnification images at day 0 and day3; (b1, c1) DAPI staining high magnification images at day 0 and day 3; (b2, c2) Live and Dead (LnD) staining high magnification images at day 0 & day 3.

Preprints (www.preprints.org) | NOT PEER-REVIEWED | Posted: 29 June 2023 doi:10.20944/preprints202306.2020.v1

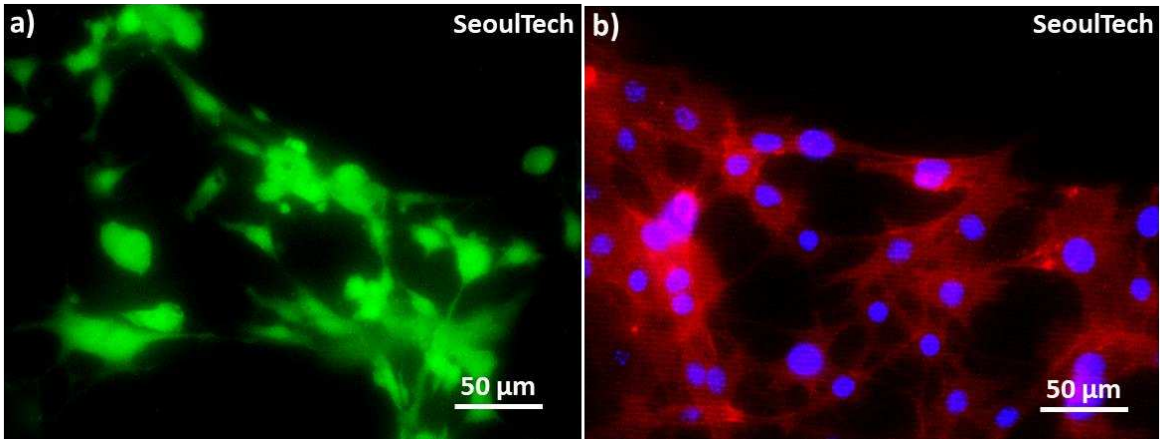

Figure 8. High magnification Live and Dead and DAPI actin images at day 3. (a) LnD image & (b) DAPI/actin image.

3. Conclusion

In this study, gelatin-hyaluronic acid based bioresponsive hydrogel crosslinked with genipin has been developed for high-density 3D bioprinting. Here, positively charged gelatin was bonded with negatively charged hyaluronic acid through polyelectrolyte complex formation. Furthermore, the free electron on the gelatin amine group reacts with the ester group at the upper end of genipin, resulting in the formation of an amide bond. This amide bond contributes to both intramolecular and intermolecular cross-linking. The bioresponsiveness of this hydrogel was evaluated in physiological conditions. These hydrogels degraded within 48 hours at 37 °C to pH 7.4 in presence of ions composed in phosphate buffer saline, whereas remain stable at room temperature for more than 5 days. Again, the gels degraded at pH 9 within 24 h but remain stable at pH 2.5 which proves the strong polyelectrolyte bond between type A gelatin and hyaluronic acid during gel formation in acidic or neutral conditions. The rheological and mechanical properties show that with the increase of gelatin content in the hydrogel, the properties increased gradually. SEM analysis showed porous morphology of the hydrogels. Successful 3D printing and four-axis printing proves that the optimized composition of hydrogel possesses excellent extrusion ability and shape fidelity properties. In vitro cell study showed the non-cytotoxicity and high cell supportiveness of this hydrogel. High density 3D bioprinting has been carried out successfully and upon the hydrogel scaffold's degradation natural ECM effects on the cell-cell communications. High cell to cell communication and formation of scaffold shape tissue would have a high potential application of this hydrogel in regenerative medicine.

4. Materials and methods

4.1. Materials

Hyaluronic acid (Kindly donated by Ildong Pharmaceutical company, Seoul, South Korea, AK0701 batch); Gelatin from porcine skin (Type A; gel strength 300), and Genipin (MW: 226.23) were purchased from Sigma Aldrich. Osteoblast cell line derived from mouse calvaria (Passage 11, MC3T3-E1 cell line, Young Science Inc., Korea), α-Minimum essential media (MEM) (Sigma Aldrich, USA), FBS (10% fetal bovine serum, Gibco Korea, Korea), penicillin-streptomycin (Sigma Aldrich, USA), LnD Max-viewTM Live/Dead cell staining kit (Biomax, Korea), 4',6-diamidino-2-phenylindole (DAPI) staining kit (Thermofisher).

4.2. Synthesis of hydrogel

0.3 g hyaluronic acid was dissolved into 10 ml distilled water (DW) by stirring overnight. After complete dissolving the solution was kept at 70°C for 2 h. Different amounts of gelatin (1 g, 1.2 g &

 doi:10.20944/preprints202306.2020.v1

1.5 g) were dissolved into 8 ml DW at 60 °C stirred for 1 h. 5 mg genipin was dissolved separately into 2 ml distilled water at room temperature. The gelatin solution was mixed with the hyaluronic acid solution by reducing the temperature to 60 °C by vigorous stirring for 1 h. After 1 h genipin solution was mixed with the HA-gelatin solution and stirred for 30 minutes. After 30 minutes, the resulting product was kept at room temperature for 3h for gelation. Table 1 shows the composition of the hydrogels and their codes used in this study.

Table 1. Different composition of gel and code. .

SI No.	Sample Composition	Sample Code
1	0.3 g HA + 1g Gelatin + 5 mg Genipin + 20 ml DW	Gel 1
2	0.3 g HA + 1.2g Gelatin + 5 mg Genipin + 20 ml DW	Gel 2
3	0.3 g HA + 1.5g Gelatin + 5 mg Genipin + 20 ml DW	Gel 3

4.3. Characterization of gelatin-HA hydrogel

Fourier transform infrared spectroscopy (FTIR) spectrometer (Varian 640-IR, ALT, USA) was carried out in lyophilized gels and raw materials in 400-4000 cm^{-1} wavelength range. R/S plus rheometer (Brookfield, USA, 25 mm diameter, parallel plates with 1 mm gap) was used to test the rheological properties of the different composition hydrogels. The experiment was done at 25 °C temperature and shear rates (0 to 100 s) according to our previous protocol [28]. A Stable Micro System (TA. XT plus texture analyzer, Surrey, UK) assessed the mechanical strength of all the gels. The gel samples were molded into a cylindrical shape of (10 mm x 10 mm) and kept in the refrigerator (~4 °C) for 24 h. In the TPA and cyclic compression test, 25% was given in the distance mode with a maximum distance of 2.5 mm (Test speed: 2 $mm.sec^{-1}$). The surface and cross section morphology of the three different composition gels were analyzed by SEM (Model: TESCAN VEGA3, Czech Republic). All samples for SEM were lyophilized and then coated with platinum sputtering.

4.4. 3D (bio) printing and four-axis printing

For 3D printing, a specialized 3D bioprinting system (SeoulTech, Korea) was implemented. As described in our previous work, the 3D complex structure was designed using Solid Works (Dassault Systems SolidWorks Corp, USA), and the G-codes for the STL files were generated using slicing software (Simplify 3D version 4.0, USA) [29,30]. The hydrogel (4 ml) was loaded into the needle-attached plastic syringe (5 ml, Musashi Engineering Inc., Korea) (22 gauge). The software was used to adjust the Z-axis (syringe holder), X-axis (stage), and Y-axis (stage) to position the syringe needle close to the substrate-bearing stage. 3D printing utilized a printing speed of 70 mm/min with a pressure of 90 kPa at room temperature (25°C).

For four-axis printing, the X, Y, and Z axis speeds were set into G-codes and controlled from the 3D printer application on the computer, the fourth axis rotation was controlled by the motor (4 rpm) connected to the rotating cylindrical polypropylene substrate, separately. A plastic tube was attached to the rotating cylindrical polypropylene substrate [31].

4.5. In vitro cytocompatibility test

The in vitro cytotoxicity of the hydrogels was evaluated using the MTT assay. The MTT assay was carried out for three days on the gel. For extraction MTT, 1 mg of each gel was kept in 1 ml of medium for 48 hours. Before the addition of extract samples to wells, 1×10^3 MC3T3-E1 cells per well were seeded on a 96-well plate and cultured under standard conditions for 24 hours. The next day, the current medium was removed and replaced by 100 µl fresh culture medium, then 10 µl of each sample extract was added to the wells for the MTT assay. The MTT assay was then done according to the previous protocol. The optical density (OD) values were measured at 570 nm. Like the previous report, the relative cell viability standardized to the control was reported (%) [25].

For cell culture studies, the 3 million/ml MC3T3-E1 cell line (passage 13) was used in preparing 3D bioprinted samples. The study was carried out into α-Minimum essential media (MEM)

containing 10% fetal bovine serum and penicillin–streptomycin (100 unit/mL) and incubated in 37◦C, 5% CO2. The *in vitro* cell culture study was performed for up to 3 days, and the samples were observed on days 0 and 3. Live/dead staining was carried out using MAX-View™ Live/Dead Cell Staining Kit, which combines green, fluorescent calcein-AM staining to show intracellular esterase activity with red-fluorescent ethidium homodimer-1 staining to confirm the loss of plasma membrane integrity. The images of the live and dead cells were taken after the addition of 1.2 µL of 2 mM ethidium homodimer-1 (EthD-1) and 0.3 µL of 4 mM calcein AM into 600 µL of phosphate-buffered saline (PBS). After the addition of the two agents, the plate was incubated in the dark for 30 min. The live and dead cells were captured using different filters present in the fluorescence microscope (Leica DMLB, Germany) and merged using the LAS- X Leica microsystems software. Samples were also stained with DAPI (4′,6-diamidino-2-phenylindole) for nucleus (blue) and rhodamine phalloidin for F-actin (red) to observe their growth and proliferation [28].

4.6. Statistical analysis

All experimental results were provided as mean ± standard deviation (S.D.) and the data was statistically compared using Origin Pro 9's ONE-WAY ANOVA. Differences were statistically significant when $p \leq 0.05$ (*) and $p \leq 0.01$ (**).

Author Contributions: M.R.K. conducted all the experiments and wrote the manuscript, A.B. analyzed data and improved the research content, M.G. did cell culture experiments, M.J. synthesized the gels for cell culture, I.N. designed the experiments and supervised the research. All authors read and approved the final manuscript.

Funding: Seoul National University of Science and Technology.

Institutional Review Board Statement: Not Applicable.

Informed Consent Statement: Not Applicable.

Data Availability Statement: The data of this study are available from corresponding author upon request.

Acknowledgments: Authors acknowledge the support from Seoul National University of Science and Technology, Seoul 01811, Republic of Korea to conduct this study.

Conflicts of Interest: The authors declare no conflict of interest.

References

1. Murphy, S.V. and A. Atala, *3D bioprinting of tissues and organs.* Nat Biotechnol, 2014. **32**(8): p. 773-85.
2. Noh, I., et al., 3D printable hyaluronic acid-based hydrogel for its potential application as a bioink in tissue engineering. Biomater Res, 2019. **23**: p. 3.
3. Murphy, S.V., A. Skardal, and A. Atala, *Evaluation of hydrogels for bio-printing applications.* J Biomed Mater Res A, 2013. **101**(1): p. 272-84.
4. Ulijn, R.V., et al., *Bioresponsive hydrogels.* Materials Today, 2007. **10**(4): p. 40-48.
5. Sgambato, A., L. Cipolla, and L. Russo, Bioresponsive Hydrogels: Chemical Strategies and Perspectives in Tissue Engineering. Gels, 2016. **2**(4).
6. Park, E., et al., Bioresponsive microspheres for on-demand delivery of anti-inflammatory cytokines for articular cartilage repair. J Biomed Mater Res A, 2020. **108**(3): p. 722-733.
7. Pourchet, L.J., et al., *Human Skin 3D Bioprinting Using Scaffold-Free Approach.* Adv Healthc Mater, 2017. **6**(4).
8. Samson, A.A.S. and J.M. Song, Scaffold-free 3D printing for fabrication of biomimetic branched multinucleated cardiac tissue construct: A promising ex vivo model for in situ detection of drug-induced sodium ion channel responses. Applied Materials Today, 2022. **27**.
9. Niazi, M., et al., Advanced Bioresponsive Multitasking Hydrogels in the New Era of Biomedicine. Advanced Functional Materials, 2021. **31**(41).
10. Vu, B., G.R. Souza, and J. Dengjel, Scaffold-free 3D cell culture of primary skin fibroblasts induces profound changes of the matrisome. Matrix Biol Plus, 2021. **11**: p. 100066.
11. Daly, A.C., M.D. Davidson, and J.A. Burdick, 3D bioprinting of high cell-density heterogeneous tissue models through spheroid fusion within self-healing hydrogels. Nat Commun, 2021. **12**(1): p. 753.

12. You, S., et al., High cell density and high-resolution 3D bioprinting for fabricating vascularized tissues. 2023. **9**(8): p. eade7923.
13. C Echave, M., et al., *Gelatin as biomaterial for tissue engineering.* 2017. **23**(24): p. 3567-3584.
14. Kirchmajer, D.M., C.A. Watson, and M.J.R.a. Ranson, *Gelapin, a degradable genipin cross-linked gelatin hydrogel.* 2013. **3**(4): p. 1073-1081.
15. Bhattacharyya, A., et al., Nanodiamond enhanced mechanical and biological properties of extrudable gelatin hydrogel cross-linked with tannic acid and ferrous sulphate. Biomater Res, 2022. **26**(1): p. 37.
16. Ouasti, S., et al., Network connectivity, mechanical properties and cell adhesion for hyaluronic acid/PEG hydrogels. Biomaterials, 2011. **32**(27): p. 6456-70.
17. Roig, F., et al., Hyaluronan based materials with catanionic sugar-derived surfactants as drug delivery systems. Colloids Surf B Biointerfaces, 2018. **164**: p. 218-223.
18. Larraneta, E., et al., Synthesis and characterization of hyaluronic acid hydrogels crosslinked using a solvent-free process for potential biomedical applications. Carbohydr Polym, 2018. **181**: p. 1194-1205.
19. Mero, A. and M. Campisi, Hyaluronic Acid Bioconjugates for the Delivery of Bioactive Molecules. Polymers, 2014. **6**(2): p. 346-369.
20. Khatun, M.R., et al., High Molecular Weight Fucoidan Loading Into and Release from Hyaluronate-Based Prefabricated Hydrogel and its Nanogel Particles Controlled by Variable Pitch and Differential Extensional Shear Technology of Advanced Twin Screw-Based System. Advanced Materials Technologies, 2022.
21. Yasin, A., et al., Advances in hyaluronic acid for biomedical applications. 2022. **10**.
22. Vasi, A.M., et al., Chemical functionalization of hyaluronic acid for drug delivery applications. Mater Sci Eng C Mater Biol Appl, 2014. **38**: p. 177-85.
23. Das, M.P., et al., Extraction and characterization of gelatin: a functional biopolymer. 2017. **9**(9): p. 239.
24. Kahoush, M., et al., Genipin-mediated immobilization of glucose oxidase enzyme on carbon felt for use as heterogeneous catalyst in sustainable wastewater treatment. Journal of Environmental Chemical Engineering, 2021. **9**(4).
25. Bhattacharyya, A., et al., Bioink homogeneity control during 3D bioprinting of multicomponent micro/nanocomposite hydrogel for even tissue regeneration using novel twin screw extrusion system. Chemical Engineering Journal, 2021. **415**.
26. A. Bigia, G. Cojazzib, S. Panzavoltaa, N. Roveria, K. Rubinia, *Stabilization of gelatin films by crosslinking with genipin.* Biomaterials. **23**(24 December 2002): p. 4827-4832.
27. Sung, H.W., et al., In vitro evaluation of cytotoxicity of a naturally occurring cross-linking reagent for biological tissue fixation. J Biomater Sci Polym Ed, 1999. **10**(1): p. 63-78.
28. Bhattacharyya, A., et al., 3D bioprinting of complex tissue scaffolds with in situ homogeneously mixed alginate-chitosan-kaolin bioink using advanced portable biopen. Carbohydrate Polymers, 2023.
29. Bhattacharyya, A., et al., Modulation of bioactive calcium phosphate micro/nanoparticle size and shape during in situ synthesis of photo-crosslinkable gelatin methacryloyl based nanocomposite hydrogels for 3D bioprinting and tissue engineering. Biomater Res, 2022. **26**(1): p. 54.
30. Tran, H.N., et al., Control of maleic acid-propylene diepoxide hydrogel for 3D printing application for flexible tissue engineering scaffold with high resolution by end capping and graft polymerization. Biomater Res, 2022. **26**(1): p. 75.
31. Janarthanan, G., S. Lee, and I. Noh, 3D Printing of Bioinspired Alginate-Albumin Based Instant Gel Ink with Electroconductivity and Its Expansion to Direct Four-Axis Printing of Hollow Porous Tubular Constructs without Supporting Materials. Advanced Functional Materials, 2021. **31**(45).